www.elsevier.nl/locate/jorganchem

Journal of Organometallic Chemistry 583 (1999) 3–10

Bis-acetonitrile(dibromo)dioxomolybdenum(VI) and derivatives: synthesis, reactivity, structures and catalytic applications☆

Fritz E. Kühn [a],*, Eberhardt Herdtweck [a], Joachim J. Haider [a],
Wolfgang A. Herrmann [a], Isabel S. Gonçalves [b,c], André D. Lopes [c], Carlos C. Romão [c]

[a] *Anorganisch-chemisches Institut der Technischen Universität München, Lichtenbergstraße 4, D-85747 Garching bei München, Germany*
[b] *Departamento de Química, Universidade de Aveiro, Campus de Santiago, 3810 Aveiro, Portugal*
[c] *Instituto de Tecnologia Química e Biológica da Universidade Nova de Lisboa, Quinta do Marquês, EAN, Apartado 127, 2780 Oeiras, Portugal*

Received 29 June 1998; received in revised form 30 July 1998

Abstract

We report on the preparation and spectroscopic properties of complexes of the general formula $MoBr_2O_2L_n$ with $L = NCCH_3$ ($n = 2$), $NCC(CH_3)_3$ ($n = 1$), NCC_6H_5 ($n = 2$). The complex $MoBr_2O_2(CH_3CN)_2$ is additionally examined by single crystal X-ray structure determination. The $MoBr_2O_2L_n$ complexes are very electron deficient (^{17}O-, ^{95}Mo-NMR evidence) and readily react with electron donor *N*-ligands to give more stable complexes e.g. $MoBr_2O_2$(bipyrimidine). The structure of the latter compound has been determined by single crystal X-ray crystallography. Reactions with organometallic complexes of the type $[Cp'Mo(CN)_2(CO)_2]K$ ($Cp' = Cp$ or Cp^*) and $Cp(CO)_2Fe(CN)$ or $[Cp(CO)Fe(CN)_2]K$ result in the immediate reduction of the Mo(VI) center, as shown by EPR spectroscopy. The $MoBr_2O_2L_n$ complexes are catalysts for the epoxidation of cyclooctene but decompose slowly during the course of the reaction due to their pronounced moisture sensitivity.

Keywords: Oxide complexes; Molybdenum complexes; Crystal structures; Olefine oxidation; N-base adducts

---

1. Introduction

Recently, we reported on bimetallic complexes between high and low oxidation state metals with nitrogen donor bridges [1]. As compounds in the high oxidation state we used rhenium oxides of the general type $XReO_3$. However, a disadvantage of such systems, especially when containing the Re(VII) complex CH_3ReO_3 (usually known as 'MTO') is the coordinative lability in donor solvents [2]. We therefore began searching for other high oxidation state transition metal systems which are known to be coordinatively more rigid. Oxomolybdenum complexes with the *cis*-MoO_2 fragment, of the general formula $MoO_2Br_2L_2$, are very important precursors or oxidation catalysts, in chemical and in biological systems [3]. Their reactivity in oxygen transfer reactions is strongly modulated by the nature of the L ligands.

As starting materials for the preparation of the desired binuclear species we prepared the nitrile complexes of the type $MoBr_2O_2L_2$ ($L = NCCH_3$ (**1**); NCC_6H_5 (**2**)) and $MoBr_2O_2(NC(CH_3)_3)$ (**3**). Despite the fact that a host of complexes of the type MoX_2O_2 is known for many years and they have been used as starting materials for numerous reactions, comparatively little is known about nitrile derivatives such as **1**–**3** [3,4]. We therefore present here a more detailed examination of these complexes, their spectroscopy, reaction chemistry, and application in the oxidation of olefins.

☆ Dedicated to Professor Dr Alberto Ceccon on the occasion of his 65th birthday.

* Corresponding author. Fax: + 89-289-13473.

E-mail address: kuehn@arthur.anorg.chemie.tu-muenchen.de (F.E. Kühn)

PII: S0022-328X(99)00102-3

2. Results and discussion

2.1. Preparation and characterization of $MoBr_2O_2L_n$ with $L = NCCH_3$, $NCC(CH_3)_3$, NCC_6H_5

2.1.1. Synthesis

The oxomolybdenum complexes used in this work, $MoBr_2O_2L_n$, are prepared as depicted in the Eq. (1). The starting material $MoBr_2O_2$ [5] is dissolved in L [$L = NCCH_3$ (**1**); NCC_6H_5 (**2**); $NCC(CH_3)_3$ (**3**)] at room temperature, and the resulting yellow solution gives the products **1**–**3** in good isolated yields within a few minutes.

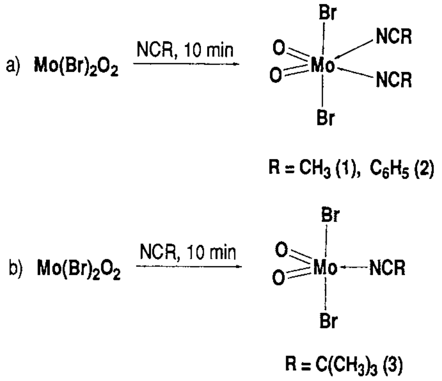

(1)

By this method a broad variety of complexes with *N* and *O* ligands is accessible to cover a wide range of electronic effects of σ donation and π acceptance [3]. Complexes **1** and **2** are distorted octahedral complexes, containing two nitrile molecules per unit (see X-ray structure of **1** below). Complex **3**, however, contains only one nitrile molecule per formula unit (as shown by elemental analysis), therefore displaying a distorted trigonal bipyramidal structure (IR evidence). This unexpected result is certainly due to the steric bulk of the *t*-butylnitrile ligand.

2.1.2. NMR-spectroscopy

The ^1H-NMR data clearly show the weak coordination of the nitrile ligands. While the complexes **1**–**3** are nearly insoluble in nonpolar, non donor solvents, e.g. alkanes or diethyl ether, they are well soluble in most donor solvents. The *t*-butylnitrile ligand increases the solubility in less polar solvents, e.g. dichloromethane or chloroform. In good donor solvents such as acetonitrile or tetrahydrofuran rapid ligand exchange can be observed.

The ^{17}O-NMR data are very similar for all three complexes. Their chemical shifts are nearly identical, showing signals around $\delta(^{17}O) \approx 1020$ ppm. The Mo(VI) center is therefore comparatively electron deficient. This might, at least partially, explain the stronger coordination to organic donor ligands in comparison to the Re(VII) systems, e.g. MTO. In the latter cases the chemical shifts, despite a strong solvent dependence, range around $\delta(^{17}O) \approx 850$ pm [6].

The ^{95}Mo-NMR data also show the signals within a narrow range around $\delta(^{95}Mo) \approx 275$ ppm. This shift also indicates a comparatively electron poor molybdenum center. It should be noted that the half widths of the signals of compound **1** and **2** is narrower than in the case of the pentacoordinated derivative **3** at room temperature both in ^{17}O- and ^{95}Mo-NMR. This may also be due to the different number of coordinating ligands and their overall steric bulk.

2.1.3. IR-spectroscopy

The C≡N stretching modes of the nitrile ligands are shifted to higher wavenumbers with respect to the free nitriles. In the case of **1** two strong C≡N absorptions are observed at 2311 and 2286 cm^{-1} (equal intensities within the accuracy of the measurement due to Fermi resonance) and a weak absorption at 2265 cm^{-1}. These vibrations are shifted to higher wavenumbers with respect to the free acetonitrile (2249 cm^{-1}) due to the coordination to the metal center. In the cases of complex **2** the two C≡N absorptions of different intensity are found at 2279 and 2231 cm^{-1}. In the case of compound **3** only one C≡N stretching vibration is observed at 2258 cm^{-1}. This finding again supports the presence of only one coordinating nitrile ligand in the case of derivative **3**. The symmetric and asymmetric Mo=O stretching vibrations of all three complexes are observed at ca. 960 and ca. 910 cm^{-1}, in a region typical for metal–oxo vibrations of this type [7].

2.1.4. X-ray crystallography

Complexes **1** and **4** (see below) were fully characterized by obtaining their crystal structures in the solid state. Details of the single crystal X-ray experiments are given in Table 1. Key bond distances and angles are listed in Table 2. Both compounds (Figs. 1(a,b) and 2(a,b)) are monomeric and belong to the general family of compounds with a $MX_2O_2N_2$ core geometry (M = transition metal). A search in the Cambridge Structural Database revealed 15 hits with 14 different molecules [8]. From the theoretical isomers (Scheme 1) one Os complex, $OsCl_2O_2py_2$ [9], matches Type C because Os has d^2 configuration here, and this compellingly leads to a *trans* arrangement of the oxo ligands. The neutral adducts $MoCl_2O_2(Me_4\text{-etda})$, $WCl_2O_2(Me_4\text{-etda})$, and $MoCl_2O_2(\eta^2\text{-TMC})$ [10] [Me_4-etda: tetramethylethylenediamine; TMC: 1,4,8,11-tetramethyl-1,4,8,11-tetraazacyclotetradecane] exhibit '*all-cis*'-geometry **A**. The majority, i.e. 10 compounds [11] together with the title compounds **1** and **4** belong to the representative type **B** and shows the halogen atoms in the apical positions of a distorted octahedron. The angle X–Mo–X ranges from 154.4° [11d] to 160.7° [11j], whereas the oxygen and nitrogen atoms define the equatorial plane together with the transition metal. However, the transition metal is off-center and shifted away from the nitrogen atoms bisecting the oxygens.

2.2. $MoBr_2O_2(CH_3CN)_2$ and its derivatives in oxidation catalysis

As already mentioned (see above) catalytic applications of Mo(VI) systems are very widespread and well examined by several groups [3,12]. Not only catalytic mechanisms in the olefin oxidation have been presented and experimentally verified, but catalytic active peroxide complexes have been isolated as well [12]. Nevertheless, we examined the catalytic behavior of complexes **1**–**3** in the catalytic oxidation of cyclooctene with *t*-butylhydroperoxide. The experimental details are given in the experimental part, a typical catalytic run is shown in Fig. 3. The reaction quickly reaches a conversion of more than 65% but does not proceed significantly further. The reason for that observation is the pronounced water sensitivity of the complexes **1**–**3**. In contrast to other more strongly coordinating organic ligands the nitriles do not prevent the moisture induced decomposition of the complexes. Therefore compounds **1**–**3** are more useful as synthetic precursors for complexes with other, more strongly coordinating or chiral ligands than as catalysts themselves.

Table 1
Crystallographic data for $MoBr_2O_2(CH_3CN)_2$ (**1**) and $MoBr_2O_2(C_8H_6N_4)$ (**4**)

	1	**4**
Empirical formula	$C_4H_6Br_2MoN_2O_2$	$C_8H_6Br_2MoN_4O_2$
Formula weight	369.85	445.91
Color/shape	Yellow/fragment	Colorless/fragment
Crystal size (mm)	0.38 × 0.20 × 0.05	0.65 × 0.38 × 0.18
Crystal system	Orthorhombic	Orthorhombic
Space group	*Pbcn*	*Pbcn*
a (pm)	897.68(5)	1672.32(9)
b (pm)	833.15(4)	1254.90(7)
c (pm)	1301.98(5)	1182.24(10)
$\alpha=\beta=\gamma$ (°)	90	90
V (10^6 pm^3)	973.75(8)	2481.0(3)
Z	4	8
T (K)	193	193
$\rho_{calc.}$ (g cm^{-3})	2.523	2.388
μ (cm^{-1})	95.1	74.9
F_{000}	688	1680
λ (pm)	71.073	71.073
Scan method	Imaging plate	Imaging plate
Θ Range (°)	3.34–25.59	2.44–27.76
Data collected (h, k, l)	±10, ±10, ±15	±21, ±16, ±15
Reflections collected	8073	25571
Independent reflections	904	2912
Reflections observed	904 (all data)	2912(all data)
Parameters refined	64	178
R_{int}	0.1464	0.0864
R_1 [a]	0.0364	0.0384
wR_2 [b]	0.0732	0.0689
Goodness-of fit [c]	1.076	0.981
Weights a/b [d]	0.0295/0.0	0.0433/0.0
$\Delta\rho_{max/min}$ (e Å^{-3})	+1.07, −1.08	+0.88, −0.77

[a] $R_1=\Sigma(||F_o|-|F_c||)/\Sigma|F_o|$.

[b] $wR_2=[\Sigma w(F_o^2-F_c^2)^2/\Sigma w(F_o^2)^2]^{1/2}$.

[c] Goodness-of fit $=[\Sigma w(F_o^2-F_c^2)^2/(\mathrm{NO}-\mathrm{NV})]^{1/2}$.

[d] $w\equiv 1/[\sigma^2(F_o^2)+(a*P)^2+b*P]$ with P: [max (0 or F_o^2)$+2F_c^2$]/3.

Table 2
Selected interatomic distances (pm) and angles (°) for $MoBr_2O_2(CH_3CN)_2$ (**1**) and $MoBr_2O_2(C_8H_6N_4)$ (**4**)

	1 [a]	**4**
Mo–Br1	251.19(4)	253.30(5)
Mo–Br2	251.19(4)	253.42(5)
Mo–O1	168.2(3)	169.3(3)
Mo–O2	168.2(3)	169.7(2)
Mo–N12	232.6(3)	232.6(3)
Mo–N22	232.6(3)	231.6(2)
N–C1	113.3(4)	
C1–C2	145.2(5)	
Br1–Mo–Br2	156.52(2)	157.67(2)
Br1–Mo–O1	96.98(9)	95.95(9)
Br1–Mo–O2	97.35(9)	96.08(9)
Br1–Mo–N12	80.93(8)	81.77(8)
Br1–Mo–N22	80.58(9)	81.94(6)
Br2–Mo–O1	97.35(9)	97.45(8)
Br2–Mo–O2	96.98(9)	96.97(9)
Br2–Mo–N12	80.58(9)	79.87(8)
Br2–Mo–N22	80.93(8)	79.66(6)
O1–Mo–O2	104.4(1)	107.0(1)
O1–Mo–N12	89.9(1)	92.5(1)
O1–Mo–N22	165.6(1)	161.4(1)
O2–Mo–N12	165.6(1)	160.4(1)
O2–Mo–N22	89.9(1)	91.6(1)
N12–Mo–N22	75.75(9)	68.82(9)

[a] The atom pairs of Br, O and N are equivalent by the symmetry operation ($-x$, y, $0.5-z$).

2.3. Reaction of organic and organometallic donor complexes with compounds **1**–**3**

Organic complexes with donor functionalities such as bipyrimidine react very quickly with complexes **1**–**3** forming octahedrally coordinated product molecules such as **4** (Eq. (2)). Both ^{95}Mo- and ^{17}O-NMR spectra of the latter compound show the higher electron density in this complex due to the donor capability of the organic ligand. However, even if reacted with a two fold or higher stoichiometric amount of complex **1**, under no circumstances are two $MoBr_2O_2$ units reacting with the bipyrimidine. The electron withdrawing effect of one $MoBr_2O_2$ unit is obviously strong enough to prevent the coordination of a second Mo(VI) unit. The same observation was made by reacting bipyrimidine

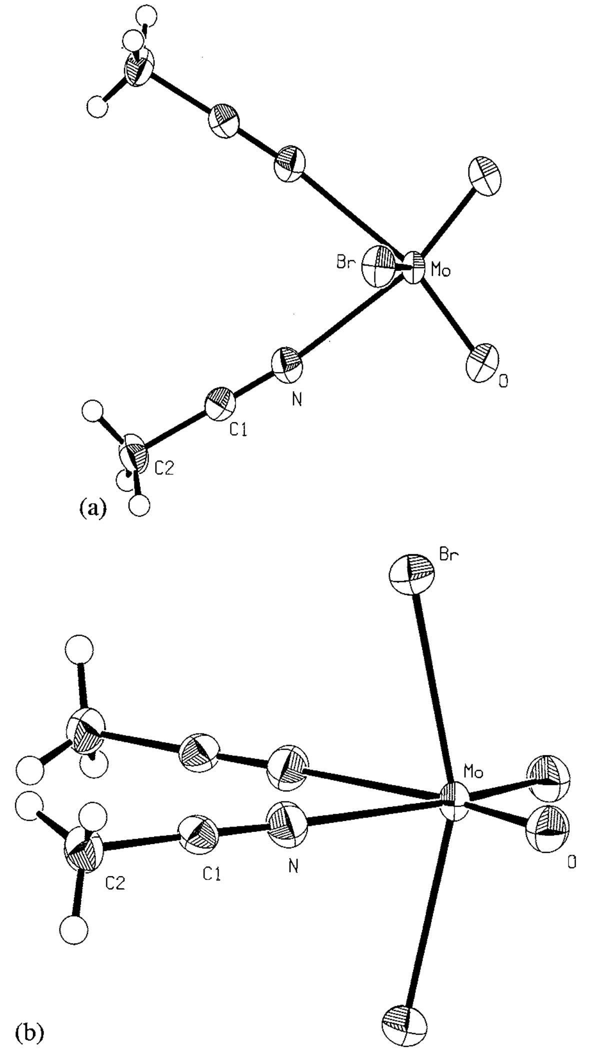

Fig. 1. ORTEP style plot of $MoBr_2O_2(CH_3CN)_2$ (**1**) with the atomic labeling scheme. Thermal ellipsoids are drawn at the 50% probability level. Hydrogen atoms are omitted for clarity. (a) Top view; (b) side view.

with excess MTO. In this case, too, only one MTO molecule is bound to the bipyrimidine unit [13]. Complex **4** was also examined by X-ray crystallography (see above).

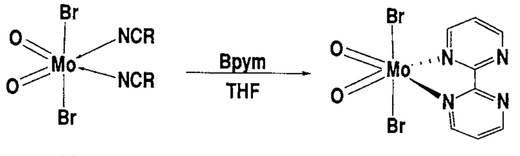

(2)

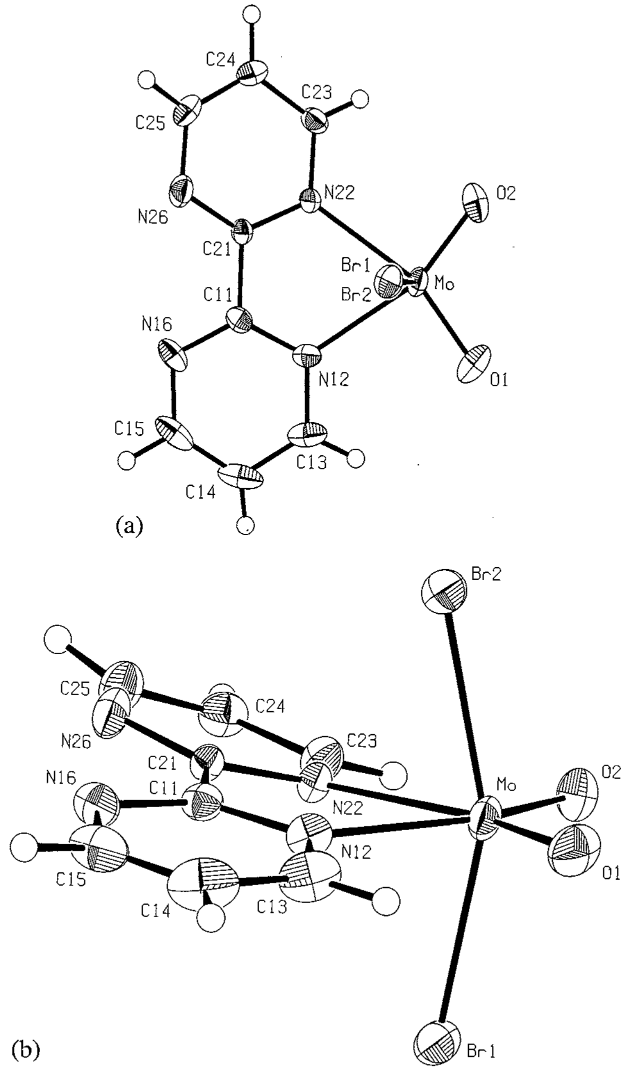

Fig. 2. ORTEP style plot of $MoBr_2O_2(bpym)$ (**4**) with the atomic labeling scheme. Thermal ellipsoids are drawn at the 50% probability level. Hydrogen atoms are omitted for clarity. (a) Top view; (b) side view.

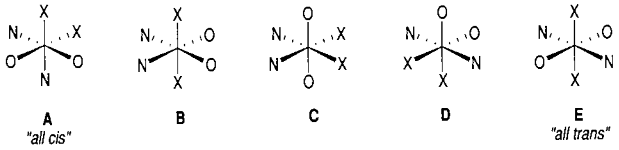

Scheme 1.

In order to enhance the donor capability of bridging bipyrimidine we combined it with an organometallic fragment. The compound $[CpMo(bpym)(CO)_2]BF_4$ (**5**) was synthesized from $CpMo(\eta^3\text{-}C_3H_5)(CO)_2$ and bipyrimidine [14]. It was then reacted with compound **1** in acetonitrile. This reaction leads to $[Cp(CO)_2\text{-}Mo(bypm)Mo(Br)_2O_2]BF_4$ (**6**) in good yields. In the product molecule **6** the ^{95}Mo-NMR signals are very broad at room temperature both in acetonitrile and nitromethane. Lowering the temperature to −20°C leads to two signals at ca. 25 ppm and at −75 ppm. The half widths of both signals are more than 2 kHz. Compound **4** displays its ^{95}Mo signal at 228 ppm, compound **5** at −80 ppm. Compound **4** clearly is already more electron rich than complex **1**. Complex **6**, however is obviously strongly influenced by the donor 'ligand' **5**, the latter giving significant electron density to the Mo(VI) center, despite its positive charge. The ^{1}H-NMR signals of the bipyrimidine ligand of complexes **4**–**6** also reflect the differences in the electron deficiency of the Mo cores. The resonances of the bipyrimidine protons of derivative **6** are observed between the downfield shifted bipyrimidine signals of complex **4** and the most upfield shifted signals of compound **5**. The Cp-ligand is only slightly influenced but is still shifted ca. 0.1 ppm downfield due to the complexation with the electron withdrawing $MoBr_2O_2$ moiety. The IR spectrum also reflects the changes due to the changed ligand surrounding of the electron deficient Mo(VI) center. While the Mo=O vibrations in complex **4** are still in the same range as for compounds **1**–**3** ($\nu = 941$ and $909\ cm^{-1}$), the vibrations of compound **6** are stronger influenced ($\nu = 973$ and $910\ cm^{-1}$). The $\nu(CO)$ IR vibrations also clearly show the difference between the coordinated Mo/Mo complexes **6** ($\nu(CO) = 1994$ and $1926\ cm^{-1}$) and the precursor compound **5** ($\nu(CO) = 1981$ and $1899\ cm^{-1}$). The product molecule is more electron deficient due to the coordination to the electron withdrawing Mo(VI) center, containing therefore a more pronounced C≡O triple bond than the more electron rich starting material. The back donating effect of the Mo orbitals to the π*-orbitals is somewhat stronger in the case of complex **5** therefore reducing the total bond order in the carbonyl slightly and weakening the C≡O bond. We additionally synthesized five more organometallic donor complexes which we intended to use as electron donors to the Mo(VI) center of the $Mo_2Br_2O_2$ moiety: $[Cp(CO)_2Mo(CN)_2]K$, $[Cp^*(CO)_2Mo(CN)_2]K$, $Cp(CO)_2Fe(CN)$, Cp(dppe)Fe(CN) and $[Cp(CO)Fe(CN)_2]K$. However, all these complexes react with the compounds **1**–**3** under immediate reduction of Mo(VI). The paramagnetism of the resulting products due to the formation of Mo(V) has been shown by EPR spectroscopy of the product complexes. A more detailed examination of these products will be presented elsewhere.

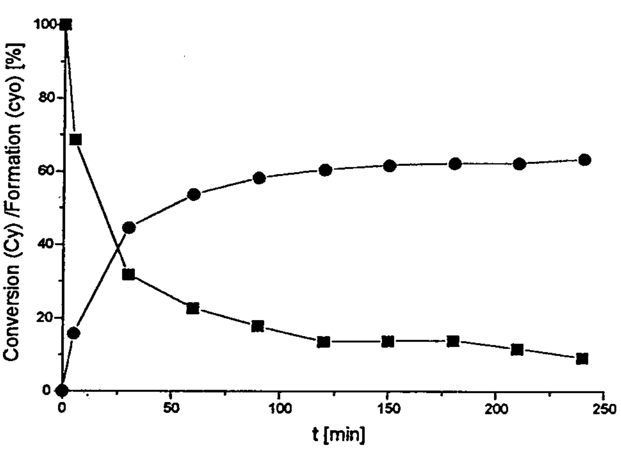

Fig. 3. Catalytic activity of $MoBr_2O_2(CH_3CN)_2$ (**1**) in the cyclooctene epoxidation. See text and experimental section for reaction details.

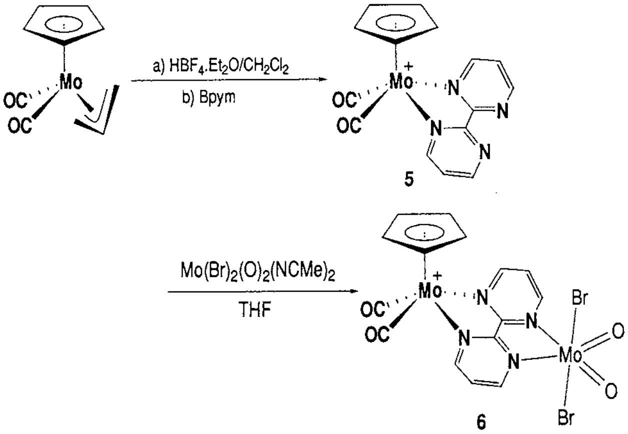

(3)

3. Conclusions

Reaction of $MoBr_2O_2$ with nitriles leads to five or six coordinated product molecules, depending on the steric bulk of the nitrile used. These product complexes are highly moisture sensitive due to the weak coordination of the nitrile ligands. They are active in the cyclooctene epoxidation but decompose because of the inevitable presence of water liberated during the reaction. Complexes **1**–**3** react readily with bipyrimidine to give a 1:1 complex. No bipyrimidine bridged species is formed because the first $MoBr_2O_2$ coordinated fragment deactivates the uncoordinated bipyrimidine N atoms. However, initial coordination of bipyrimidine to a low oxidation state Mo(II) complex allows for the formation of a high-low oxidation state bimetallic complex with a bipyrimidine bridge which is able to convey the mutual electronic influences between both metal centres. Similar attempts to make high-low oxidation state bimetallic complexes with cyanide bridges, which has been successfully achieved with $XReO_3$ complexes, failed with $MoBr_2O_2$ due to its strong oxidation behavior.

4. Experimental

4.1. Materials and procedures

All preparations and manipulations were performed with standard Schlenk techniques under an oxygen-free and water-free argon atmosphere. Solvents were dried by standard procedures THF, Et_2O, pentane, and hexane over Na/benzophenone ketyl; acetonitrile and dichloromethane were distilled after refluxing several hours over P_2O_5. Acetone was distilled over K_2CO_3 and kept over 4 Å molecular sieves.

Microanalyses were performed at ITQB (Oeiras) and the TU Munich. ^{1}H-NMR spectra were obtained with a Bruker CXP 300 spectrometer and a Bruker Avance DPX-400 spectrometer, ^{13}C-NMR spectra were measured at 100.28 MHz on a JEOL JNM GX-400 and a Bruker Avance DPX-400, ^{95}Mo-NMR and ^{17}O-NMR spectra were measured at 26.07 and 54.14 MHz, respectively, on a Bruker Avance DPX-400. Infrared spectra were recorded on a Unican Mattson Mod 7000 FTIR spectrophotometer and a Perkin-Elmer FT-IR spectrometer using KBr pellets and/or solutions.

The precursor materials $Mo(Br)_2(O)_2$ [5] $[Cp^*(CO)_2Mo(NCMe)_2][BF_4]$ [15], $[Cp(CO)_2Mo(CN)_2]K$ [1a, 16], $Cp(CO)_2Fe(CN)$ [16], Cp(dppe)Fe(CN) [17], $[Cp(CO)Fe(CN)_2]K$ [16] were prepared as described previously.

4.2. Preparation of complexes of general formula $MoBr_2O_2L_n$ [L = NCMe (**1**) (n = 2); NCC_6H_5 (**2**) (n = 2), $NCC(CH_3)_2$ (**3**) (n = 1)]

To the powder $Mo(Br)_2(O)_2$ (0.75 g, 1.03 mmol) were added L [L = NCMe (**1**); NCC_6H_5 (**2**); $NCC(CH_3)_2$ (**3**)] (20 ml), and the solution turned yellow. After 10 min the solution was filtered and evaporated to dryness. Yield: 90% **1**; 92% **2**; and 96% **3**.

$MoBr_2O_2(NCMe)_2$ (**1**): Anal. Found: C 12.93; H 1.66; N 7.41. Calc. for $C_4H_6Br_2MoN_2O_2$ (369.85): C 12.99; H 1.64; N 7.57%. Selected IR data: (Nujol, ν cm^{-1}): 2311 s, 2286 s, 2265 w, 1030 s, 953 vs, 938 s, 910 vs, 795 s, 723 s, 581 m; NMR-Data: ^{1}H (d_8-THF, 400 MHz, 20°C) δ(ppm) = 1.98 (s); ^{17}O(d_8-THF, 20°C) δ(ppm) = 1024 ($\Delta\nu_{1/2}$ = 176 Hz); ^{95}Mo (d_8-THF, 20°C) δ(ppm) = 275 ($\Delta\nu_{1/2}$ = 183 Hz).

$MoBr_2O_2(NCC_6H_5)_2$ (**2**): Anal. Found: C 33.91; H 2.08; N 5.52; Br 32.37. Calc. for $C_{14}H_{10}Br_2MoN_2O_2$ (494.00): C 34.04; H 2.04; N 5.67, Br 32.35%. Selected IR (Nujol, ν cm^{-1}): 2279 s, 2231 w, 1532 m, 1238 s, 1208 s, 964 vs, 910 vs, 868 vs, 818 s, 733 s, 698 m, 665 m, 584 m; NMR data: ^{1}H (d_8-THF, 400 MHz, 20°C) δ(ppm) = 7.71 (2H, m), 7.64 (1H, m), 7.50 (2H, m); ^{17}O(d_8-THF, 20°C) δ(ppm) = 1020 ($\Delta\nu_{1/2}$ = 204 Hz); ^{95}Mo (d_8-THF, 20°C) δ(ppm) = 279 ($\Delta\nu_{1/2}$ = 203 Hz).

$MoBr_2O_2(NCC(CH_3)_3)$ (**3**): Anal. Found: C 15.93; H 2.34; N 3.44; Br 42.81. Calc. for $C_5H_9Br_2MoNO_2$ (370.88): C 16.19; H 2.45; N 3.78, Br 43.09%. Selected IR (Nujol, ν cm^{-1}): 2729 m, 2258 s, 1593 m, 1307 m, 1198 m, 1173 m, 1022 m, 953 vs, 914 vs, 841 s, 752 vs, 731 s, 677 m, 550 m; NMR data: ^{1}H (d_8-THF, 400 MHz, 20°C) δ(ppm) = 1.31 (s); ^{17}O(d_8-THF, 20°C) δ(ppm) = 1021 ($\Delta\nu_{1/2}$ = 437 Hz); ^{95}Mo (d_8-THF, 20°C) δ(ppm) = 278 ($\Delta\nu_{1/2}$ = 366 Hz).

4.3. Preparation of $MoBr_2O_2$(bipyrimidine) (**4**)

A solution of $MoO_2Br_2(NCMe)_2$ (0.15 g, 0.39 mmol) in THF (15 ml) was treated with bipyrimidine (0.06 g, 0.39 mmol) and the mixture was vigorously stirred for 20 min. The resulting yellow solution was evaporated to dryness and a pale yellow microcrystalline power was formed. Yield: 92%. Anal. Found: C 21.39; H 1.39; N 12.59, Br 35.68. Calc. for $C_8H_6Br_2MoN_4O_2$ (445.91): C 21.55; H 1.36; N 12.56, Br 35.84%. Selected IR data: (KBr, ν cm^{-1}): 3080 m, 2961 m, 2930 m, 2885 w, 1725 m, 1636 m, 1576 s, 1555 s, 1452 m, 1409 vs, 1302 m, 1211 m, 1103 m, 1016 m, 941 vs, 909 vs, 820 s, 755 s, 691 m, 660 s; NMR data: ^{1}H-NMR (CD_3CN, 400 MHz, 20°C) δ (ppm) = 9.65 (d, 2H), 9.29 (d, 2H), 7.90 (m, 2H); ^{17}O-NMR (CD_3CN, 20°C) δ (ppm) = 997 ($\Delta\nu_{1/2}$ = 160 Hz); ^{95}Mo-NMR (CD_3CN, 20°C) δ (ppm) = 227.8 ($\Delta\nu_{1/2}$ = 100 Hz).

4.4. Preparation of $[Cp(CO)_2Mo(bipyrimidine)]BF_4$ (**5**)

A solution of $CpMo(\eta^3-C_3H_5)(CO)_2$ (0.45g, 1.74 mmol) in dichloromethane (15 ml) was treated with bipyrimidine (0.29g, 4.50 mmol). After vigorous stirring for 1h the resulting mixture was evaporated to dryness. The violet microcrystalline complex was washed with ether, n-pentane and dried in vacuum. Yield: 91%. Anal. Found: C 39.17; H 2.53; N 12.34. Calc. for $C_{15}H_{11}BF_4MoN_4O_2$ (462.03): C 39.00; H 2.40; N 12.13%. Selected IR data: (Nujol, ν cm^{-1}): 3108 m, 2960 w, 2935 w, 2880 w, 1981 vs, 1899 vs, 1578 s, 1406 s, 1082 s, 1058 s, 853 m, 809 m, 527 m, 477 m; NMR data: ^{1}H-NMR (CD_3CN, 400 MHz, 20°C) δ (ppm) = 9.28 (d, 2H), 9.15 (d, 2H), 7.66 (t, 2H), 5.96 (s, 5H, Cp); ^{95}Mo-NMR (CD_3CN, 20°C), δ (ppm) = −79.7 ($\Delta\nu_{1/2}$ = 80 Hz).

4.5. Preparation of $[\{Cp(CO)_2\text{-}Mo(bipyrimidine)\}\text{-}MoBr_2O_2]BF_4$ (**6**)

A solution of $MoO_2Br_2(NCMe)_2$ (0.18 g, 0.48 mmol) in THF (10 ml) was treated $[Cp(CO)_2Mo(bpym)]BF_4$ (0.22 g, 0.48 mmol). After 30 min the dark violet solution was concentrated to ca. 5 ml and addition of diethyl ether precipitated the product. The mother liquor was filtered off and the remaining precipitate was washed with diethyl ether/*n*-pentane and dried in vacuum. Yield: 82%. Anal. Found: C 23.79; H 1.29; N 7.82; Br 21.59. Calc. for $C_{15}H_{11}BBr_2F_4Mo_2N_4O_4$ (749.77): C 24.03; H 1.48; N 7.47, Br 21.31%. Selected IR data: (KBr, ν cm^{-1}): 3088 m, 2962 w, 2940 w, 2870 w, 1994 vs, 1926 vs, 1579 m, 1409 s, 1202 m, 1056 s, 973 s, 910 m, 820 m, 799 w, 729 s, 520 m, 471 m; NMR-Data: ^{1}H (d_8-THF, 400 MHz, 20°C) δ(ppm) = 9.50 (m, 4H), 7.85 (m, 2H), 5.90 (m, 5H); ^{95}Mo (d_8-THF, 20°C) δ(ppm) = 25 ($\Delta\nu_{1/2}$ = 2400 Hz), −75 ($\Delta\nu_{1/2}$ = 2100 Hz).

4.6. Preparation of $[Cp^*(CO)_2Mo(CN)_2]K$ (**7**)

A solution of $[Cp^*Mo(NCMe)_2(CO)_2][BF_4]$ (0.54 g, 1.18 mmol) in methanol/ethanol (5/10) was reacted with excess of KCN (0.29 g, 4.50 mmol) and the mixture was vigorously stirred for 6 h. The resulting orange solution was filtered, evaporated to dryness, extracted with acetone and concentrated. Upon addition of n-pentane an oily residue was separated which was solidified to a yellow microcrystalline powder after scratching and repeated washings with pentane. Yield: 86%. Anal. Found: C 44.65; H 4.11; N 7.63. Calc. for $C_{14}H_{15}KMoN_2O_2$ (378.33): C 44.45; H 4.00; N 7.40%. Selected IR data: (Nujol, ν cm^{-1}): 2097 s, 2089 s, 1946 vs, 1861 vs, 1462 s, 1377 s, 723 m; NMR data: ^1H-NMR (CD_2Cl_2, 300 MHz, 20°C) δ (ppm) = 1.20 (s, 15H, Cp*); ^{95}Mo-NMR (CD_2Cl_2, 20°C) δ (ppm) = − 1421 ($\Delta\nu_{1/2} = 130$ Hz).

*4.7. Catalytic reactions with compounds **1–3** as catalysts*

cis-Cyclooctene (800 mg, 7.3 mmol), 800 mg *n*-dibutylether (internal standard), 1 mol% (73 μmol) **1–3** (as catalyst), and 2 ml 5.5 M *tert*-butylhydroperoxide in decane were added to a thermostated reaction vessel and stirred for 4 h at 55°C.

The course of the reaction was monitored by quantitative GC-analysis. Samples were taken every thirty minutes, diluted with chloroform, and chilled in an icebath. For the destruction of hydroperoxide and removal of water a catalytic amount of manganese dioxide and manganese sulfate was added. After the gas evolution ceased the resulting slurry was filtered over a filter equipped Pasteur pipette and the filtrate injected in the GC column.

The conversion of cyclooctene and formation of cyclooctene oxide was calculated from a calibration curve ($r^2 = 0.999$) recorded prior to the reaction course.

5. X-ray crystallography

5.1. General procedure

Suitable single crystals for the X-ray diffraction studies were grown by standard techniques from saturated solutions of compound **1** in $NCCH_3/Et_2O$ and derivative **4** in *n*-pentane/*n*-hexane/$(CH_3)_2O/Et_2O$ at room temperature. Both structures were solved by a combination of Patterson methods, difference-Fourier syntheses and full-matrix least-squares refinements. Neutral atom scattering factors for all atoms and anomalous dispersion corrections for the non-hydrogen atoms were taken from International Tables for X-Ray Crystallograpy. All calculations were performed on a DEC 3000 AXP workstation with the STRUX-V system, including the programs PLATON, PLUTON, SHELXS-86, SHELXL-93, and SIR-92 [18].

*5.2. Data collection, structure solution and refinement for the complexes (**1**/**4**).*

A summary of the crystal and experimental data is reported in Table 1. Preliminary examination and data collection were carried out on an imaging plate diffraction system (IPDS; Stoe&Cie) equipped with a rotating anode (NONIUS FR591; 50/50 kV; 60/80 mA; 3.0/4.0 kW) and graphite monochromated Mo–K_α radiation. Data collections were performed at 193 K within the Θ-range of $3.34° < \Theta < 25.59°/2.44° < \Theta < 27.76°$ with an exposure time of 120 s per image (rotation scan modus from $\varphi = 0.0$ to 217° with $\Delta\varphi = 1°$). A total number of 8073/25571 reflections were collected. 713/1622 systematic absent reflections were rejected from the original data set. After merging a sum of 904 independent reflections remained and were used for all calculations. Data were corrected for Lorentz and polarization effects. Corrections for absorption and decay effects were applied with the program Decay [18g,h]/PLATON (option: difabs) [18c]. A correction for extinction effects was applied for compound **1**. The unit cell parameters were obtained by full-matrix least-squares refinements of 4374/4868 reflections with the program Cell [18g,h]. All 'heavy atoms' of the asymmetric unit were anisotropically refined. Hydrogen atoms were found in the difference maps and refined with individual isotropic thermal displacement parameters. Full-matrix least-squares refinements were carried out by minimizing $\Sigma\, w(F_o^2 - F_c^2)^2$ with SHELXL-93 weighting scheme and stopped at shift/err < 0.001.

6. Supplementary material

Crystallographic data (excluding structure factors) for the structure(s) reported in this paper have been deposited with the Cambridge Crystallographic Data Centre as supplementary publication no. CCDC–118934 (**1**), and CCDC–118935 (**4**). Copies of the data can be obtained free of charge on application to CCDC, 12 Union Road, Cambridge CB2 1EZ, UK (fax: (+ 44)1223-336-033; e-mail: deposit@ccdc.cam.ac.uk).

Acknowledgements

This work was supported by PRAXIS XXI, Project (2/2.1/QUI/419/94). The authors want to thank the DAAD and CRUP (INIDA and Acções Integradas Programme) for generous support. ADL (BD) thanks PRAXIS XXI for a grant, FEK acknowledges the Alexander von Humboldt foundation for financial support. Professor J. Mink is acknowledged for helpful discussions.

References

[1] (a) M.G.B. Drew, V. Félix, I.S. Gonçalves, F.E. Kühn, A.D. Lopes, C.C. Romão, Polyhedron 17 (1998) 1091. (b) I.S. Gonçalves, F.E. Kühn, A.D. Lopes, J. Parola, F. Pina, J. Sotomayor, C.C. Romão, J. Organomet. Chem. 560 (1998) 117.

[2] (a) C.C. Romão, F.E. Kühn, W.A. Herrmann, Chem. Rev. 97 (1997) 3197. (b) W.A. Herrmann, F.E. Kühn, Acc. Chem. Res. 30 (1997) 169.

[3] (a) S.B. Kumar, M. Chaudhury, J. Chem. Soc. Dalton Trans. (1991) 2169. (b) P. Palanca, T. Picher, V. Sanz, P. Gómez-Romero, E. Llopis, A. Domenech, A. Cervilla, J. Chem. Soc. Chem. Comm. (1990) 531. (c) J.P. Wilshire, L. Leon, P. Bosserman, D.T. Sawyer, J. Am. Chem. Soc. 101 (1979) 3379. (d) J.M. Berg, R.H. Holm, J. Am. Chem. Soc. 107 (1985) 925. (e) J.P. Caradonna, E.W. Harlan, R.H. Holm, J. Am. Chem. Soc. 108 (1986) 7856. (f) F.J. Feher, K. Rahimian, T.A. Budzichowski, J.W. Ziller, Organometallics 14 (1995) 3920. (g) R. Clarke, M. Gahagan, R.K. Mackie, D.F. Foster, D.J. Cole-Hamilton, M. Nicol, A.W. Montford, J. Chem. Soc. Dalton Trans. (1995) 1221. (h) J.R. Backhouse, H.M. Lowe, E. Sinn, S. Suzuki, S. Woodward, J. Chem. Soc. Dalton Trans. (1995) 1489. (i) U. Piarulli, D.N. Williams, C. Floriani, G. Gervasio, D. Viterbo, J. Chem. Soc. Dalton Trans. (1995) 3329.

[4] (a) J.J. Berzelius, Adv. Phys. Lpz. 46 (1826) 381. (b) W. Puttbach, Liebigs Ann. 201 (1880) 125. (c) O. Ruff, F. Eisner, Ber. dt. Chem. Ges. 38 (1905) 742. (d) I.A. Glukov, R.A. Rodionova, Dokl. Akad. Naukl. Talzhik SSR 2 (1959) 15. (e) C.W. Blomstrand, J. Prakt. Chem. 77 (1859) 89. (f) F.F. Smith, V. Oberholtzer, J. Am. Chem. Soc. 15 (1893) 26.

[5] R. Colton, J.B. Tomkins, Austr. J. Chem. 18 (1965) 447.

[6] (a) W.A. Herrmann, F.E. Kühn, P.W. Roesky, J. Organomet. Chem. 485 (1995) 243. (b) W.A. Herrmann, F.E. Kühn, M.U. Rauch, J.D.G. Correia, G. Artus, Inorg. Chem. 34 (1995) 2914. (c) F.E. Kühn, J. Haider, E. Herdtweck, W.A. Herrmann, A.D. Lopes, M. Pillinger, C.C. Romão, Inorg. Chim. Acta. 279 (1998) 44.

[7] W.P. Griffith, J. Chem. Soc. A (1969) 211.

[8] (a) 3D Search and Research Using the Cambridge Structural Database. F.H. Allen, O. Kennard, Chem. Des. Automat. News 8 (1993) 1 and 31–37. (b) 181 309 entries; search on $[\mathrm{Tr}^{\mathrm{CN}^{6}}(=\mathrm{O})2(\cdots \mathrm{X})2(\cdots \mathrm{N})2]$

[9] (a) W.A. Herrmann, S.J. Eder, W. Scherer, Chem. Ber. 126 (1993) 39. (b) Y. Imbe, K. Umakoshi, C. Matsunami, Y. Sasaki, Inorg. Chem. 34 (1995) 813.

[10] (a) K. Dreisch, C. Andersson, C. Stalhandske, Polyhedron 12 (1993) 303. (b) A. Lachgar, P. Farrall, J.M. Mayer, Polyhedron 12 (1993) 2603. (c) K. Dreisch, C. Andersson, C. Stalhandske, Polyhedron 11 (1992) 2143.

[11] (a) R.H. Fenn, J. Chem. Soc. A (1969) 1764. (b) See Dreisch et al., Ref. [10a]. (c) W.A. Herrmann, W.R. Thiel, E. Herdtweck, Chem. Ber. 123 (1990) 271. (d) I. Sens, H. Stenger, U. Müller, K. Dehnicke, Z. Anorg. Allg. Chem. 610 (1992) 117. (e) B. Viossat, N. Rodier, Acta Crystallogr. Section B 35 (1979) 2715. (f) D.M. Baird, F.L. Yang, D.J. Kavanaugh, G. Finness, K.R. Dunbar, Polyhedron 15 (1996) 2597. (g) Sang-Oh Oh, Seong-Jong Mo, J. Korean Chem. Soc. 39 (1995) 318. (h) L. Arnaudet, R. Bougon, B. Ban, P. Charpin, J. Isabey, M. Lance, M. Nierlich, J. Vigner, Can. J. Chem. 68 (1990) 507. (i) V.S. Sergienko, V.L. Abramenko, M.A. Porai-Koshits, A.D. Garnovskii, Zh. Strukt. Khim. 31 (1990) 45. (j) H. Arzoumanian, G. Agrifoglio, H. Krentzien, M. Capparelli, J. Chem. Soc. Chem. Comm. (1995) 655.

[12] (a) W.R. Thiel, M. Angstl, N. Hansen, J. Mol. Catal. A Chem. 103 (1995) 5. (b) W.R. Thiel, T. Priermeier, Angew. Chem. 107 (1995) 1870; Angew. Chem. Int. Ed. Engl. 34 (1995) 1737. (c) W.R. Thiel, T. Priermeier, T. Bog, J. Chem. Soc. Chem. Comm. (1995) 1871. (d) W.R. Thiel, T. Priermeier, D. Fiedler, A.M. Bond, M.R. Mattner, J. Organomet. Chem. 514 (1996) 137. (e) W.R. Thiel, Chem. Ber. 129 (1996) 575. (f) I. Hatzopoulos, W.R. Thiel, H.-D. Brauer, J. Photochem. Photobiol. A: Chem. 102 (1997) 151. (g) W.R. Thiel, J. Mol. Catal. A Chem. 117 (1997) 449.

[13] W.A. Herrmann, R. Alberto, G.R.J. Artus, unpublished results.

[14] (a) J.R. Ascenso, I.S. Gonçalves, E. Herdtweck, C.C. Romão, J. Organomet. Chem. 508 (1996) 169. (b) M.J. Calhorda, C.A. Gamelas, I.S. Gonçalves, E. Herdtweck, C.C. Romão, L. Veiros, Organometallics 17 (1998) 2597.

[15] (a) J.R. Ascenso, C.G. de Azevedo, I.S. Gonçalves, E. Herdtweck, D.S. Moreno, M. Pessanha, C.C. Romão, Organometallics 14 (1995) 3901. (b) I.S. Gonçalves, Ph.D. Dissertation, Technical University of Lisbon (1996).

[16] C.E. Coffey, J. Inorg. Nucl. Chem. 25 (1963) 179.

[17] P.M. Treichel, D.C. Molzahn, Synth. React. Inorg. Met. Org. Chem. 9 (1979) 21.

[18] (a) A.J.C. Wilson (Ed.), International Tables for Crystallography, Vol. C, Tables 6.1.1.4 (pp. 500–502), 4.2.6.8 (pp. 219–222), and 4.2.4.2 (pp. 193–199), Kluwer, Dordrecht, The Netherlands, 1992. (b) G.R. Artus, W. Scherer, T. Priermeier, E. Herdtweck, 'STRUX-V', A Program System to Handle X–ray Data, TU München, Germany, (1997). (c) A.L. Spek, PLATON-PLUTON, An Integrated Tool for the Analysis of the Results of a Single Crystal Structure Determination, Acta Crystallogr. Section A 46 (1990) C34. (d) G.M. Sheldrick, SHELXS-86, A Program for the Solution of Crystal Structures from Diffraction Data, Acta Crystallogr. Section A 46 (1990) 467. (e) G.M. Sheldrick, SHELXL-93, in: G.M. Sheldrick, C. Krüger, R. Goddard (Eds.), Crystallographic Computing 3, pp. 175–189, Oxford University Press, London, 1993. (f) A. Altomare, G. Cascarano, C. Giacovazzo, A. Guagliardi, M.C. Burla, G. Polidori, M. Camalli, SIR-92, University Bari, Italy, 1992. (g) IPDS Operating System Version 2.8. Stoe&Cie. GmbH, Darmstadt, Germany (1995). (h) W. Schütt, E. Herdtweck, F. Hahn, and F.R. Kreißl, J. Organomet. Chem. 443 (1993) C33 and references cited therein.